

## Electrodynamic Containment of Charged Particles

R. F. WUERKER, H. SHELTON, AND R. V. LANGMUIR\*  
*Ramo-Wooldridge Research Laboratory, Los Angeles 45, California†*  
 (Received August 1, 1958; revised September 2, 1958)

Electrically charged iron and aluminum particles having diameters of a few microns have been contained in a confined region of space by means of alternating and static electric fields. The theory is essentially that of alternating gradient focusing; here the motion is governed by Mathieu's equation. Under certain circumstances when many particles are confined the three dimensional focusing force and the Coulomb repulsion results in a "crystalline" array which can be "melted" and reformed.

**S**TUDIES in this laboratory on the electrical charging in vacuum of small dust particles resulted in the development of a method of containing these particles in dynamic equilibrium by alternating electric fields.<sup>1,2</sup> This new technique is based upon the strong focusing principle which has as its analogue the classical problem of the upside-down pendulum. Essentially this device can be thought of as a closed form of W. Paul's and M. Raether's electric mass filter.<sup>3</sup> The new variation can be employed to suspend any charged particle (e.g., charged dust, ions, electrons, etc.) in dynamic equilibrium.<sup>4</sup>

The necessary condition for the proper operation of this type of suspension system depends upon finding electrode configurations which give sinusoidally time varying forces whose strengths are proportional to the distance from a central origin. Under this condition, the differential equation of particle motion is a special case of the Mathieu differential equation. A three dimensional electrical configuration which satisfies this requirement is the circularly symmetric potential distribution

$$V = \left[ \frac{V_{dc} - V_{ac} \cos \Omega t}{z_0^2} \right] \left[ z^2 - \frac{r^2}{2} \right], \quad (1)$$

where  $V_{ac}$  is the peak value of the alternating signal of angular frequency  $\Omega$  applied in series with the constant voltage  $V_{dc}$ . Differentiation shows that the field intensities have the required space dependence and are

$$E_z = 2(-V_{dc} + V_{ac} \cos \Omega t) \frac{z}{z_0^2} \quad (2)$$

and

$$E_r = -(-V_{dc} + V_{ac} \cos \Omega t) \frac{r}{z_0^2}. \quad (3)$$

The negative 2:1 ratio between the variation with distance of fields in the two directions shows that when the electric field is focusing toward the origin in the  $z$  direction then it must be defocusing in the  $r$  direction and vice versa.

The differential equations of a motion of particle of charge-to-mass ratio  $e/m$  in this potential field are

$$\frac{d^2 z}{dt^2} = - \left( \frac{e}{m} \right) \left( \frac{2V_{dc}}{z_0^2} \right) z + \left( \frac{e}{m} \right) \left( \frac{2V_{ac}}{z_0^2} \right) z \cos \Omega t, \quad (4)$$

and

$$\frac{d^2 r}{dt^2} = + \left( \frac{e}{m} \right) \left( \frac{V_{dc}}{z_0^2} \right) r - \left( \frac{e}{m} \right) \left( \frac{V_{ac}}{z_0^2} \right) r \cos \Omega t. \quad (5)$$

The equations of motion of a single particle in the two directions of space are seen to be identical except for the negative 2:1 ratio between the constants. Equation (4) is a function of  $z$  only while (5) is a function of  $r$  only. The motions in  $z$  and  $r$  are therefore mutually independent. Each of the above equations is thus a special case of the Mathieu differential equation which in its general form is usually written

$$\frac{d^2 u}{dx^2} + (a - 2q \cos 2x)u = 0 \quad (6)$$

in which  $u$  may represent either  $z$  or  $r$ . The dimensionless constants in the above equation are related to those of the present physical problem through the transformation equations

$$x = \Omega t / 2, \quad (7)$$

$$a_z = -2a_r = 8 \left( \frac{e}{m} \right) \left( \frac{V_{dc}}{z_0^2} \right) \frac{1}{\Omega^2}, \quad (8)$$

and

$$q_z = -2q_r = 4 \left( \frac{e}{m} \right) \left( \frac{V_{ac}}{z_0^2} \right) \frac{1}{\Omega^2}. \quad (9)$$

Clearly motion with negative  $q$  is the same as with positive  $q$  except for a change of phase of the drive. Physically the Mathieu differential equation demonstrates that when the alternating driving force  $2q$

\* California Institute of Technology. Consultant to Ramo-Wooldridge.

† A division of Thompson-Ramo-Wooldridge Company.

<sup>1</sup> Shelton, Wuerker, and Langmuir, *Bull. Am. Phys. Soc. Ser. II*, **2**, 375 (1957).

<sup>2</sup> H. C. Corben, *Bull. Am. Phys. Soc. Ser. II*, **2**, 375 (1957).

<sup>3</sup> W. Paul and M. Raether, *Z. Physik* **140**, 262-273 (1955).

<sup>4</sup> It is understood that Professor W. Paul has independently been conducting similar experiments on the containment of atomic particles (unpublished).

vanishes the particle will oscillate with a natural harmonic motion of frequency equal to  $(a)^{\frac{1}{2}}$ .

The Mathieu Eq. (6) is solvable in an infinite series

$$u = A e^{\mu x} \sum_{n=-\infty}^{\infty} C_{2n} \epsilon^{i2nz} + B \epsilon^{-\mu x} \sum_{n=-\infty}^{\infty} C_{2n} \epsilon^{-i2nz} \quad (10)$$

in which the quantities  $\mu$  and  $C_{2n}$  are functions of the parameters  $a$  and  $q$ . The exponent  $\mu$  in the above equation is all important in that it determines the two different types of solutions. Thus if  $\mu$  is either a real or complex number the amplitude builds up exponentially and the particle is not stably bound. If on the other hand  $\mu = i\beta$  the motion is bounded and the particle remains in dynamic equilibrium. For stable containment the quantity  $\beta x$  is related to the frequency of the dominant term in the series solution, and, as pointed out earlier, it is equal to  $(a)^{\frac{1}{2}}$  when  $q$  is zero. Thus, for the present physical problem  $\beta x$  is related to the fundamental frequency of particle motion in the two orthogonal directions  $\omega_z = \beta_z x/t$  and  $\omega_r = \beta_r x/t$ . Using the transformation Eq. (7) between the normalized independent variable ( $x$ ) and time ( $t$ ) gives the fundamental frequencies in the two directions as a function of their respective  $\beta$ 's and the driving frequency  $\Omega$ , i.e.,  $\omega_z = \beta_z \Omega/2$  and  $\omega_r = \beta_r \Omega/2$ . Accordingly  $\beta$  or its implied  $\omega$  will be referred to as the "resultant frequency of motion."

It can be shown that the particle will be stably bound if the values of  $a$  and  $q$  are within the region bounded by the curves

$$a = -\frac{1}{2}q^2 + \frac{1}{128}q^4 - \frac{29}{2304}q^6 + \frac{68687}{188\,74368}q^8 \quad (11)$$

(corresponding to the special case of  $\beta=0$ ), and

$$a = 1 - q - \frac{1}{8}q^2 + \frac{1}{64}q^3 - \frac{1}{1536}q^4 - \frac{11}{35864}q^5 + \dots \quad (12)$$

(corresponding to  $\beta=1$ ).<sup>5</sup>

The question of the range of  $a$ - $q$  values necessary for the stable confinement of a particle in three dimensions can be represented by plotting Eqs. (11) and (12) for the  $r$  and  $z$  direction of the cylindrical coordinate system on a single Cartesian graph. Figure 1 shows the resulting "necktie" stability plot for the axially symmetric potential distribution of Eq. (1). The stable  $a_z$ ,  $a_r$ ,  $q_z$ , and  $q_r$  values are contained within the solid boundary curves (corresponding to  $\beta_r=0$ ,  $\beta_r=1$ ,  $\beta_z=0$ , and  $\beta_z=1$ ) which have been drawn through the theoretical values.<sup>6</sup> The points and curves within the

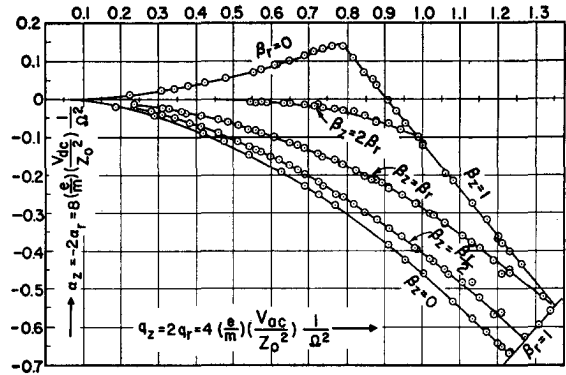


FIG. 1. Normalized stability diagram for the axially symmetric electrodynamic suspension system. The solid line passes through the theoretical values. The three curves within the region of stability are the experimentally determined loci along which the resultant motions are, respectively, in the following ratios  $\beta_r/\beta_z=2, 1$ , and  $\frac{1}{2}$ . The probable error is indicated by the size of the circles.

region of stable operation represent experimentally determined values which will be fully described later.

Operation of the present system is specified in  $a$ - $q$  space by a straight line intercepting the origin and of slope

$$a/q = 2V_{dc}/V_{ac}. \quad (13)$$

That is to say, for given applied voltages  $V_{dc}$  and  $V_{ac}$  this operational line determines the range of driving frequency  $\Omega$  through which a particle of given  $e/m$  will be stably bound. Conversely if the frequency is also held constant the  $a/q$  operational line specifies the range of  $e/m$  values which will be accepted (i.e., higher  $e/m$  particles correspond to higher  $q$  values). Thus it can be seen that by properly adjusting the ratio of the two voltages so that the operational line just passes one of the edges of the stability curve the  $e/m$  acceptance of the chamber can be made quite narrow. It is with a similar operation that Professor W. Paul made his channel device into a sensitive mass spectrometer.<sup>3</sup>

When no direct voltage is added in series with the drive the operation of the system is specified along the abscissa ( $a=0$ ) of Fig. 1. Solution of Eq. (12) for  $a=0$  shows that the maximum value of  $q$  for stability is  $q_{max}=0.908$ ; hence the minimum applied driving frequency according to Eq. (9) is

$$\Omega_z \min = 1.484 \left[ \left( \frac{e}{m} \right) \left( \frac{2V_{ac}}{z_0^2} \right) \right]^{\frac{1}{2}}. \quad (14)$$

The evaluation of this expression for the specific case of  $2V_{ac}/z_0^2 = 1000$  v/cm<sup>2</sup> is presented in Table I in order to illustrate range of frequencies encountered with particles of different charge-to-mass ratios. The theory further predicts the existence of other narrow regions of bounded operation, corresponding to values of  $\beta > 1$ , but to date the existence of these higher modes has not been experimentally verified.

<sup>5</sup> N. W. McLachlan, *Theory and Applications of Mathieu Functions* (Oxford University Press, New York, 1947).

<sup>6</sup> The values for Eqs. (11) and (12) were taken from published tables. Computation Laboratory, U. S. Bureau of Standards, *Tables Relating to Mathieu Function* (Columbia University Press, New York, 1951).

TABLE I.

| (2V <sub>ac</sub> /z <sub>0</sub> <sup>2</sup> = 1000 v/cm <sup>2</sup> )                                    |                              |                                    |
|--|------------------------------|------------------------------------|
| Particle   | e/m<br>coulombs/<br>kilogram | f = Ω <sub>min</sub> /2π<br>cy/sec |
| Electron   | 1.76 × 10 <sup>11</sup>      | 313 Mc                             |
| Proton   | 9.6 × 10 <sup>7</sup>        | 7.31 Mc                            |
| Uranium 238  | 4.05 × 10 <sup>6</sup>       | 478 Kc                             |
| 20-μ diam aluminum particle carrying<br>0.35 million units of elementary<br>charge, and thus charged to 51 v | 0.005                        | 53 cy/sec                          |

The preceding paragraphs have summarized some of the mathematical methods and salient results obtained from Mathieu equation theory. As with many such nonlinear problems, physical intuition is easily lost in the mathematical manipulations. A simplified approximate solution when β and q are small has been found which helps one more easily to comprehend the physical principles governing the operation of the electrodynamic suspension system. Referring again to Eq. (6) we assume that the particle position as represented by z can be separated into two components

$$z = Z + \delta \tag{15}$$

such that δ, the smaller component, is a displacement of small amplitude governed by the periodically varying applied driving force 2q, while Z describes the average value of the displacement over a complete period of the drive. Z will change much more slowly, but with a larger amplitude than δ, and its values define the resultant motion. Thus the solution, when stable, will consist of a slow vibration upon which is superimposed a smaller ripple due to the drive. Substitution of Eq. (15) into the Mathieu equation enables one to effect a simplification under the assumption that δ ≪ Z, but dδ/dt ≫ dZ/dt

$$\frac{d^2\delta}{dx^2} = -(a - 2q \cos 2x)Z. \tag{16}$$

If a ≪ q the above equation is easily integrated under the assumed relative constancy of Z

$$\delta = -\frac{qZ}{2}(\cos 2x) \tag{17}$$

demonstrating that when the particle is stably bound the micromotion is 180° out of phase with the drive. Substitution of Eqs. (17) and (15) back into the original differential equation gives

$$\frac{d^2z}{dx^2} = -aZ + \frac{aqZ}{2} \cos 2x + 2qZ \cos 2x - q^2Z \cos^2 2x. \tag{18}$$

The resultant acceleration, d<sup>2</sup>Z/dx<sup>2</sup>, is found by averaging

the instantaneous acceleration over a cycle of the drive

$$\frac{d^2Z}{dx^2} = \frac{d^2z}{dx^2} = \frac{1}{\pi} \int_0^\pi \frac{d^2z}{dx^2} dx = -\left(a + \frac{q^2}{2}\right)Z. \tag{19}$$

Under the assumed approximations, the apparent motion has been reduced to a differential equation of harmonic motion, and our approximate theory shows that the particle will vibrate stably with a resultant dimensionless frequency of motion of

$$\beta = \left[ \left(a + \frac{q^2}{2}\right) \right]^{1/2}. \tag{20}$$

In the special case of a = 0 the particle will vibrate in the potential field of Eq. (1) with resultant frequency of motion of

$$\omega_z = \beta_z \Omega / 2 = \sqrt{2} \left(\frac{e}{m}\right) \left(\frac{V_{ac}}{z_0^2}\right) \left(\frac{1}{\Omega}\right) \frac{\text{radians}}{\text{second}} \tag{21}$$

and

$$\omega_r = \beta_r \Omega / 2 = \frac{1}{\sqrt{2}} \left(\frac{e}{m}\right) \left(\frac{V_{ac}}{z_0^2}\right) \left(\frac{1}{\Omega}\right) \frac{\text{radians}}{\text{second}}. \tag{22}$$

These approximations are valid when q ≲ 0.4. The 2:1 ratio between the two frequencies of resultant motion correspond to the 2:1 ratio between the electric field strengths in the two orthogonal directions. In the absence of series dc voltage and for small values of q the particle is expected to vibrate in a characteristic 2:1 Lissajous pattern.

The addition of direct voltage in series with the drive strengthens the effective binding in one direction at the expense of the other with the result that the resultant vibrational frequencies will be correspondingly altered. For example, the application of a series voltage which results in a force toward the axis along the r direction acts to make up for the inherent geometrical weakness in this direction. Thus it is expected that the proper addition of a series voltage can cause the particle to vibrate with equal resultant motions in both directions (i.e., ω<sub>z</sub> = ω<sub>r</sub>), and the trajectory will have the over-all appearance of a 1:1 or circular Lissajous pattern. The approximate theory shows that this condition will occur when a<sub>z</sub> = -q<sub>z</sub><sup>2</sup>/4. A further increase in r focusing will increase the resultant frequency of motion in the r direction while decreasing the resultant frequency in the z direction, and one finds a condition in which the particle will vibrate on the average twice as fast in the r direction as in the z direction (i.e., ω<sub>r</sub> = 2ω<sub>z</sub>). The particle trajectory then will have the appearance of a 1:2 Lissajous pattern. The approximate theory shows that this condition will occur when a<sub>z</sub> = -5q<sub>z</sub><sup>2</sup>/12. Further increase in r focusing will eventually cause the static field to exactly cancel out the binding effect of the driving frequency in the z direction (i.e., ω<sub>z</sub> = 0). On setting β = 0 in Eq. (20) it is seen, referring back

to Eq. (11), that the approximate analysis has given the first term in the expression for the lower boundary of stability.

We have seen that the electrodynamic suspension system is able to compete against anharmonic forces (corresponding to negative values of  $a$ ) and still maintain a particle in equilibrium. The case of uniform forces such as gravity or constant electric fields will now be considered. Such forces modify the original Mathieu differential equation giving

$$\frac{d^2z}{dx^2} + (a - 2q \cos 2x)z = A \tag{23}$$

where  $A$ , the normalized constant force, is related to the physical problem by

$$A = 4F/m\Omega^2, \tag{24}$$

the physical force being represented by  $F$ . The complete solution of this differential equation is the sum of the particular integral corresponding to  $A$  and the complementary function [Eq. (10)]. However, by using the approximate solution outlined in the previous paragraphs one is able to obtain an approximate expression for the particular integral in closed form; namely

$$\frac{d^2Z}{dx^2} + \left(a + \frac{q^2}{2}\right)Z = A. \tag{25}$$

The normalized solution of this equation is

$$Z = B \sin \left\{ \left(a + \frac{q^2}{2}\right)^{\frac{1}{2}} x \right\} + \frac{A}{[a + (q^2/2)]}. \tag{26}$$

It may be seen that the uniform force displaces the center of motion by an amount proportional to its magnitude and inversely proportional to the square of the resultant frequency of motion. In the present

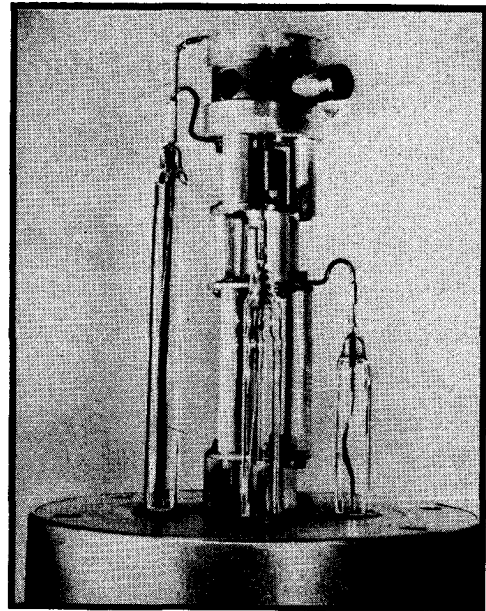


FIG. 3. Photograph of the experimental electrodynamic suspension system.

physical problem this displacement is

$$\Delta = F/m\omega_z^2. \tag{27}$$

If this displacement is equal to the dimensions of the apparatus establishing the potential field, the particle is lost. For example if the force is due to gravity the particle can "fall out" when the resultant frequency of motion becomes too small. Gravity will accordingly slightly alter the appearance of the lower stability curves of Fig. 1.

**EXPERIMENTAL ELECTRODYNAMIC SUSPENSION APPARATUS**

A small experimental chamber which gave the required potential distribution was machined out of aluminum. This, in turn, was mounted above an electric powder injector, and the whole apparatus was mounted within a vacuum envelope. Figure 2 shows schematically the complete apparatus with the electrical circuit through which the driving voltage ( $V_{ac}$ ), the series voltage ( $V_{dc}$ ), and the "uniform" voltage  $V_g$  are applied to the trapping chamber. As can be seen, the driving signal is applied between the end caps and the annular ring by a variable dc voltage and ac audiogenerator. In addition, means were provided for applying an alternating voltage  $V_\beta$  across the end caps for the purpose of experimentally measuring the resultant frequency of motion in the  $z$  direction. As shown, ports were drilled in the caps and the ring electrode for the purpose of microscopically examining the interior, introducing the dust particles, the particle charging current, and the carbon arc illumination. Figure 3 shows a photograph of the apparatus as it is mounted

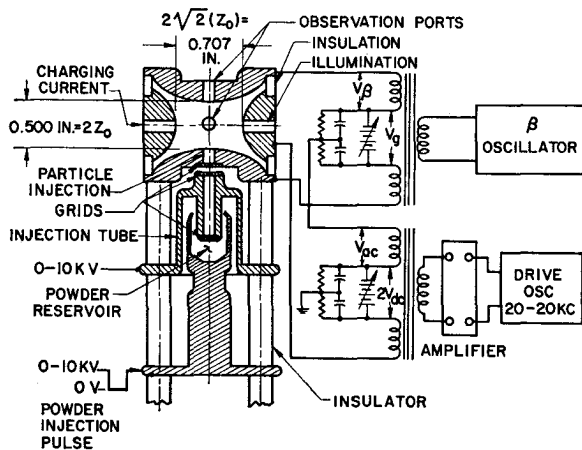


FIG. 2. Schematic diagram of the electrodynamic suspension system.

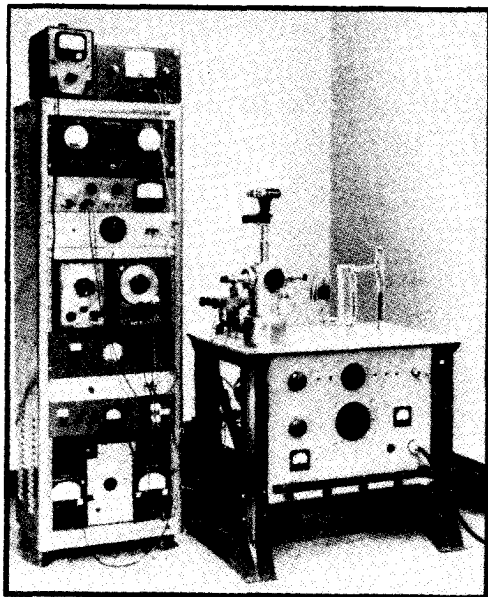


FIG. 4. Photograph of the complete apparatus for studying the electrodynamic suspension of charged dust particles.

upon the vacuum face plate. These components are contained in turn within a brass vacuum envelope which mounts the microscope tubes, the illumination port, and the charging gun. (See Fig. 4.)

The experimental operation of the suspension system is as follows: first the chamber is evacuated to a pressure less than  $20 \mu$  of Hg, the driving signal is applied between the ring and end caps (initially the driving frequency is around 150 cy/sec with an amplitude of  $V_{ac}/\sqrt{2} = 500$  v rms), the carbon arc illuminator is struck, and the charging current is turned on. The chamber is then ready to accept the powder which is

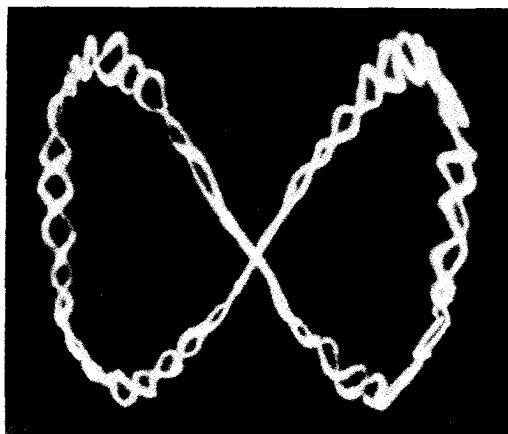


FIG. 5. Retouched microphotograph of the 2:1 Lissajous trajectory in the  $r$ - $z$  plane of a single charged particle of aluminum dust contained by the electrodynamic suspension system.  $V_{ac} = 500$  v rms,  $V_{dc} = 0$ ,  $\Omega/2\pi = 200$  cy/sec, and  $\omega_s/2\pi = 16.3$  cy/sec. One calculates from these experimentally measured values:  $e/m = 0.0053$  coulombs/kg,  $a_s = 0$ ,  $q_s = 0.232$ , and  $\beta_s = 0.163$ .

injected into the interior by pulsing the bucket of the injector to ground potential for a few milliseconds through a thyatron circuit. Observation perpendicular to the axis of the chamber through the horizontal microscope enables one to observe visually a contained particle which has been charged by the beam and is bobbing around the interior of the chamber under the confining influence of the alternating electric fields. Figure 5 shows a photomicrograph of a charged piece of aluminum dust (around  $20 \mu$  diam) when  $a/q = 0.7$ . It will be noted that the trajectory is a 2:1 Lissajous pattern upon which is superimposed the driving frequency.

As expected from the theoretical analysis, the addition of voltage ( $V_a$ ) across the end caps displaces the particles either up or down depending upon the polarity and sign of charge of the particle. By properly

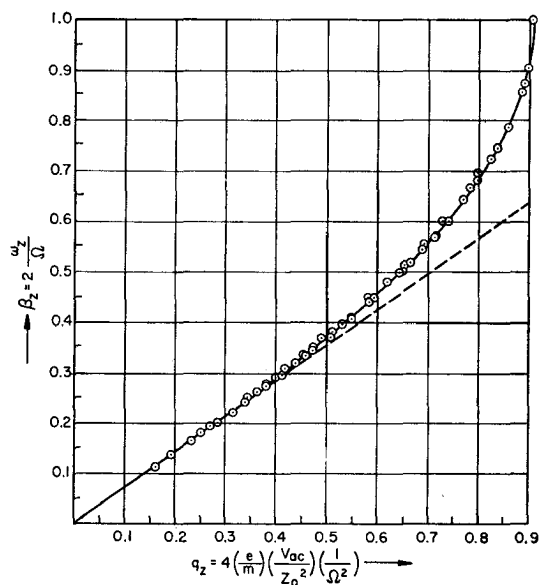


FIG. 6. The normalized resultant frequency of motion  $\beta$  as function of  $q$  when  $a = 0$ .

adjusting this voltage gravity can be canceled out, the sign of the charge of the particle can be determined and the  $e/m$  ratio can be estimated [using Eq. (27)]. When gravity is neutralized the driving frequency can be extended to very high values without having the particle fall out of the chamber. By applying a small alternating voltage ( $V_\beta$ ) of approximately 0.1 v rms across the end caps using a second oscillator the resultant frequency of motion in the  $z$  direction can be measured by visually observing when the particle motion is in resonance with the applied signal. A small difference between the two frequencies results in an easily observed beat frequency which disappears when

<sup>7</sup> The photomicrographs were taken with a Leitz MIKAS 35-mm microscope camera using Kodak Tri-X film. The speed of film was increased by developing the negatives with FR X-500 Developer. Exposure times were typically between  $\frac{1}{16}$ – $\frac{1}{8}$  sec.

the two are exactly equal. At resonance the orbit elongates by an amount determined by the background vacuum pressure. Figure 6 shows the experimental measurements of the normalized resultant frequency of  $z$  motion as a function of the parameter  $q$  when  $V_{dc}=0$  (i.e.,  $a/q=0$ ). These data were obtained by varying both the driving frequency and driving voltage. Inspection of this graph shows that the approximate theory begins to fail by more than 1% when  $q \gtrsim 0.4$ .

The product of the resultant frequency of motion and drive frequency is directly proportional to the product of the charge to mass ratio and the gradient of the driving field intensity in the  $z$  direction in accordance with Eq. (20). This simplified relationship enables one to measure accurately the charge to mass ratio of the particle knowing the driving voltage and chamber dimensions. As the driving frequency is progressively decreased, the resultant motion speeds up, the ripple due to drive becomes more prominent, and finally the

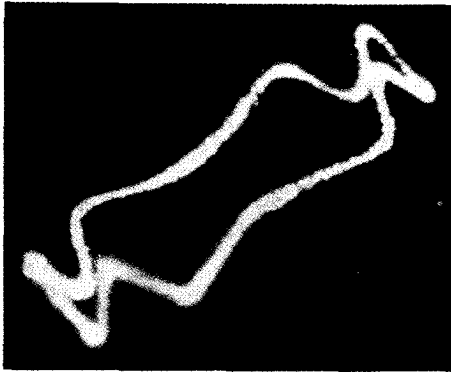


FIG. 7. Retouched microphotograph of a 1:1 Lissajous Trajectory in the  $r-z$  plane.  $V_{ac}=500$  v rms,  $2V_{dc}=-90.2$  v,  $\Omega=148$  cy/sec, and  $e/m=0.00625$  coulombs/kg. One calculates from these experimental values that  $q_z=0.502$ ,  $a_z=-0.0643$ , and  $a_z/q_z=-0.128$ .

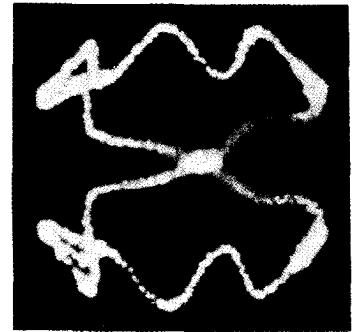
motion builds up in the  $z$  (vertical) direction and the particle is thrown out of the chamber.

Measurement of the frequency of the "upper region of stability" gives a third way of estimating the charge to mass ratio of the particle using Eq. (14).

The addition of voltage ( $V_{dc}$ ) in series with the drive  $V_{ac}$  enables one to explore experimentally the full region of stable operation of this suspension system as mapped in Fig. 1. Figure 7 shows a microphotograph of a single particle trajectory which is like a 1:1 Lissajous pattern. Figure 8 shows the 1:2 Lissajous pattern obtained by further increasing the series voltage ( $V_{dc}$ ). Figure 9 shows the "perverse" trajectory down deep within the region of stable operation.

The experimental points on the boundary curves of the stability diagram are plotted in Fig. 1. It was possible to measure a point without loss of the charged particles by careful manipulation of the voltages and frequency and by recognizing when the motion was on

FIG. 8. Retouched microphotograph of a 1:2 Lissajous trajectory viewed in the  $r-z$  plane.  $V_{ac}=500$  v rms,  $2V_{dc}=-144$  volts,  $\Omega=148$  cy/sec, and  $e/m=0.00625$  coulombs/kg gram. One calculates from these experimental values that  $q_z=0.502$ ,  $a_z=-0.102$ , and  $a_z/q_z=-0.204$ .



the verge of no longer being stable. Besides experimentally tracing out the region of stable operation, one can further determine the loci of points where the resultant motions in the two directions are in 2:1, 1:1, and 1:2 ratios as seen in Fig. 1. The determination of these curves becomes a little difficult for large values of  $q$ .

In essence, using single particles, the above apparatus can be employed as an analogue computer of the Mathieu differential equation. It should be mentioned that once a particle is trapped within the chamber it stays. Some have been held in suspension for as long as a weekend.

### Containment of Many Particles

Besides verifying the theory concerning the containment of a single particle the electrodynamic suspension system also showed that it could compete against interparticle Coulomb forces. Experimentally it was found that when the powder was initially injected and charged, instead of accepting a single particle the chamber filled up with many. This behavior in fact was the more usual case. At first the motions were quite violent and mixed up; however, on dissipating the initial kinetic energies by increasing the background pressure to several microns the particles could be made to take up stable arrays. Arrays of more particles than could easily be counted have been seen.

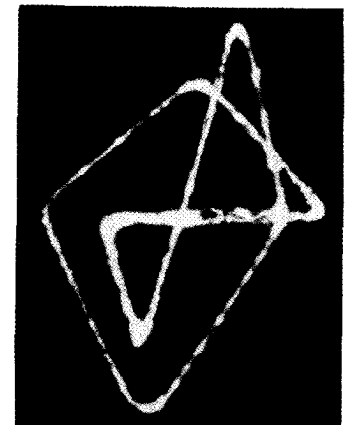


FIG. 9 Retouched microphotograph of a single particle trajectory viewed in the  $r-z$  plane deep within the region of stable operation.  $V_{ac}=500$  v rms  $2V_{dc}=-269$  volts,  $\Omega=92.5$  cycles/second, and  $e/m=0.00623$  coulomb/kg. The values of the normalized parameters are  $q_z=1.29$ ,  $a_z=-0.49$ , and  $a_z/q_z=-0.38$ .

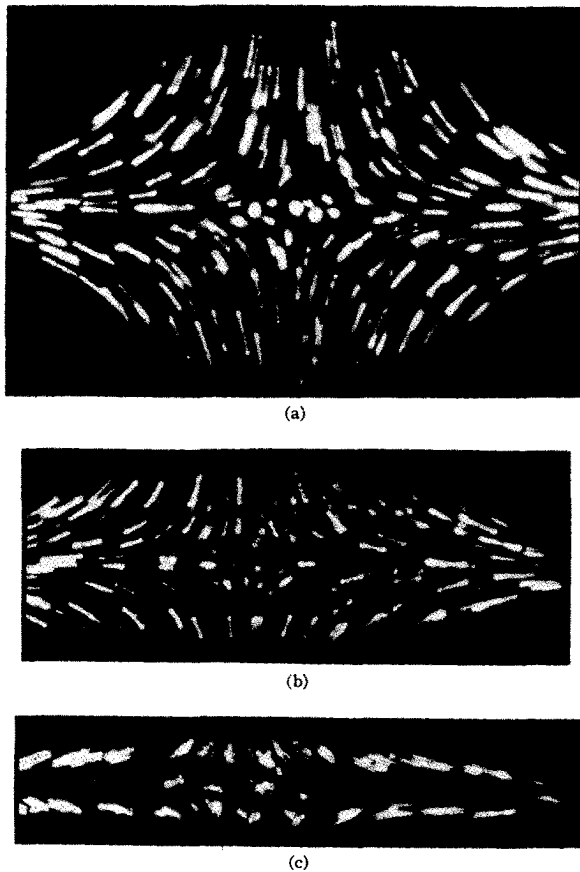


FIG. 10. Many body suspension viewed in the  $r$ - $z$  plane. Experimental values:  $V_{ac}=500$  v rms,  $\Omega=210$  cy/sec. (a) Top picture:  $2V_{dc}=-30$  v,  $\omega_z=21.7$  cy/second; (b) Middle picture:  $2V_{dc}=0$ ,  $\omega_z=26.0$  cy/sec; (c) Bottom picture:  $2V_{dc}=+24.7$  v,  $\omega_z=29.4$  cy/sec. The average charge to mass ratio of a single particle was  $e/m=0.00765$  coulombs/kg.

In Fig. 10 the effect, as seen in the  $r$ - $z$  plane, of the series voltage ( $V_{dc}$ ) on a typically stable array of positively charged aluminum particles can be seen. Each line corresponds to a single particle which is vibrating about its stable position under the influence of the alternating field. One notes that on proceeding away from the center the amplitude of vibration increases. The orientation of the individual particle vibrations serves to map out the electric field pattern within the chamber. Most interesting is the effect of varying either the driving frequency or the driving voltage. If the frequency is increased (or conversely  $V_{ac}$  decreased) the "cloud" of particles expands to a new equilibrium. If on the other hand the frequency is decreased the array is compressed. As the drive is further decreased the array is progressively compressed and the individual particle motions get larger. At some point (which is a function of the vacuum pressure) the static array "melts" and the particles again move around in a random fashion in large orbits. If the frequency is increased the particles "recrystallize." The process of "melting and recrystallization" can be repeated over and over again. The time of "recrystallization" is a function of the number of particles, background pressure, and the amplitude and frequency of the drive. If the pressure is quite high (around  $5$ - $10$   $\mu$ ) and the frequency also large ( $q < 0.2$ ) the recrystallization time will be of the order of seconds. If, conversely, the pressure is lowered to around  $0.1$   $\mu$  then the static array may take many minutes to re-establish itself.

The array of Fig. 10 is unique due to its symmetry (gravity in this case was canceled out by the application of  $V_g=20$  v). In most cases a wide range of  $e/m$  is

TABLE II.

| $\frac{\Omega}{2\pi} \frac{B}{\text{cy/sec}}$ | Number of particles       |                           |                           |                           |       |                              |
|---|---------------------------|---------------------------|---------------------------|---------------------------|-------|------------------------------|
|   | $\sim 100$                | 32                        | 5                         | 3                         | 2     | 1 $q$                        |
| 210   | 0.248                     | 0.229                     | 0.220                     | 0.220                     | 0.221 | 0.221-0.307                  |
| 200   | 0.272                     | 0.257                     | 0.247                     | 0.248                     |       | 0.246-0.339                  |
| 190   | 0.305                     | 0.284                     | 0.275                     | 0.273                     | 0.273 | 0.273-0.376                  |
| 180   |                           | 0.319                     | 0.309                     | 0.309                     |       | 0.304-0.418                  |
| 170   | 0.390                     | 0.362                     | 0.347                     | 0.347                     | 0.345 | 0.347-0.469                  |
| 160   |                           | 0.415                     | 0.400                     | 0.400                     | 0.400 | 0.396-0.530                  |
| 150   | 0.530                     | 0.481                     | 0.465                     | 0.465                     |       | 0.456-0.602                  |
| 145   |                           |                           | 0.503                     | 0.504                     |       | 0.645                        |
| 140   | melts<br>at 143<br>cy/sec |                           |                           |                           |       |                              |
| 135   |                           | 0.579                     | 0.555                     | 0.551                     | 0.547 | 0.545-0.691                  |
| 130   |                           | 0.645                     | 0.610                     | 0.609                     |       | 0.603-0.744                  |
|   |                           | melts<br>at 131<br>cy/sec |                           |                           |       |                              |
| 125   |                           |                           | 0.692                     | 0.690                     | 0.692 | 0.680-0.801                  |
|   |                           |                           | melts<br>at 125<br>cy/sec |                           |       |                              |
|   |                           |                           |                           | 0.806                     | 0.799 | 0.785-0.866                  |
|   |                           |                           |                           | melts<br>at 122<br>cy/sec |       | unstable-0.907<br>121 cy/sec |

accepted and the static pattern has the appearance of a stalactite with the particles of high  $e/m$  on top and those of progressively lower  $e/m$  ratios dangling below. The high  $e/m$  particles can be rejected by decreasing the frequency until they are unstable or conversely the low  $e/m$  particles dropped out by increasing the frequency. By using the series voltage ( $V_{ac}$ ) as described in the theory only particles within a narrow band can be kept.

Using the second oscillator the resonance frequency of the cloud can be investigated by observing when the particles absorb energy. Starting with the uniform cloud of Fig. 10 the frequency was measured as a function of the drive—also the “melting frequency” was noted. After a run was completed some particles were

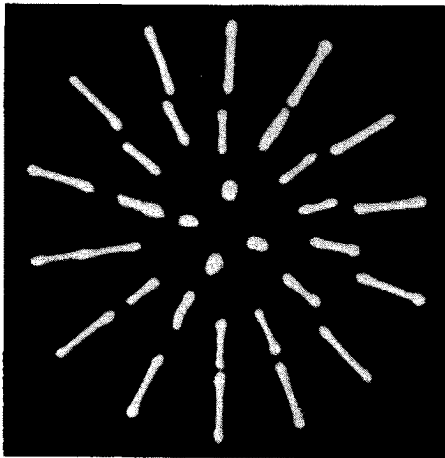


FIG. 11. Suspension of 32 positively charged particles viewed in the  $r-\theta$  plane.  $V_{ac}=500$  v rms,  $2V'=0$ ,  $\Omega=135$  cy/sec,  $\omega_z=43.6$  cy/sec. The average charge to mass ratio of a single particle was  $e/m=0.00765$  coulomb/kg.

thrown out of the chamber and a new run taken by changing the frequency. This process was repeated progressively until only one particle was left. Table II shows the experimental results. It is seen that for a given drive “ $\beta$ ” is a function of the number of particles. The values  $q$  listed on the right were computed from the one particle data.

Figure 11 shows a microphotographic view in the  $r-\theta$  plane of the 32 particles for which data were taken in Table II. This top view is typical of the observed “crystalline” arrays of many particles. Figure 12 shows

FIG. 12. Suspension of five positively charged particles viewed in the  $r-\theta$  plane.  $V_{ac}=500$  v rms,  $2V_{dc}=0$ ,  $\Omega=210$  cy/sec, and  $\omega_z=23.1$  cy/sec. The charge to mass ratio of a single particle was later found to be  $e/m=0.00765$  coulomb/kg.



a top view of the five particles for which data were taken in Table II. Note that each particle lies at apex of a regular pentagon. In the three particle case the particles were bound in an equilateral triangle in  $r-\theta$  plane.

Besides containing particles of only one sign we have seen the simultaneous containment of particles of both sign. In this case when  $V_a$  is added across the top caps the particles are caused to move vertically in opposite directions.

#### HIGH-FREQUENCY-EXCITATION

The audio source used in the previously described work was replaced by a 300 megacycle source which theoretically would confine electrons. Experiment demonstrated that excitation by the high frequency resulted in the production of a visible glow inside the chamber. The vacuum was such that an electron mean-free path was about 1000 times the chamber dimensions. The glow could be extinguished by addition of dc voltage in series with the driving signal. Details of this work will be reported at a later date.‡

#### ACKNOWLEDGMENTS

We wish to thank Dr. David B. Langmuir and Dr. H. C. Corben for their many helpful discussions and encouragement. Also we want to thank Mr. Richard L. Young for his assistance in the construction of some of the equipment and making some of the measurements, and Mrs. Virginia Gannon for her assistance in the preparation of the manuscript.

‡ *Note added in proof.*—The following references have recently come to our attention: (a) M. L. Good, Univ. Calif. Rad. Lab. Report No. 4146 (1953). Declassified (1956). (b) Fisher, Osberg-haus, and Paul, Forschungsber. Wirtsch. Ministeriums Nordrhein Westfalen, No. 415 (1958). (c) Paul, Reinhard, and von Zahn, Z. Physik 152, 143–182 (1958). (d) E. Fisher, thesis, University of Bonn (unpublished) (1958).